Journal of Physics:
Conference Series

PAPER • **OPEN ACCESS**

Theoretical and experimental analysis of the impact of a recuperative stage on the performance of an ORC-based solar microcogeneration unit

To cite this article: Fabio Fatigati *et al* 2023 *J. Phys.: Conf. Ser.* **2648** 012008

Theoretical and experimental analysis of the impact of a recuperative stage on the performance of an ORC-based solar microcogeneration unit

Fabio Fatigati [1], Arianna Coletta, Roberto Carapellucci and Roberto Cipollone

Department of Industrial and Information Engineering and Economics, University of L'Aquila, Piazzale Ernesto Pontieri, Monteluco di Roio, 67100, L'Aquila, Italy

Abstract. Microgeneration ORC-based units driven by solar energy, which enable combined heat and power generation (CHP), are a promising solution for decarbonizing the domestic sector. However, the intermittent availability of solar energy, coupled with the variability in user demand for domestic hot water (DHW), can lead the system to frequent off-design conditions and a less reliable energy supply. Consequently, increasing attention has recently been focused on the technological and design solutions for improving plant performance and ensuring its continuous operation. This paper presents the results of an experimental campaign carried out to investigate the possible advantages – in terms of efficiency and savings of thermal energy in the upper source – of introducing a recovery heat exchanger (RHX) in the basic configuration of a solar ORC-based system. Tests were conducted on a fully instrumented ORC-based plant with two 12 kW electric heaters providing the thermal power recovered through the solar collectors. The RHX is introduced into a recuperative branch that can be bypassed by closing a dedicated three-way valve. The study aims to investigate the behavior of the ORC unit in the absence of solar radiation (with the electric heaters switched off) when the recovery unit is powered only by the hot water stored in the Thermal Energy Storage (TES) tank. Another purpose of the present work is to evaluate the benefits introduced by the RHX in reducing the temperature decrease of the TES hot water and, consequently, maximizing the operating time of the ORC-based unit. In order to support the experimental analysis, a comprehensive theoretical model of the unit was developed and validated against experimental data. The model was used as a software platform to optimize the plant design and recuperative branch configuration. The theoretical model was developed in the GT-Suite™ environment thus integrating a mono and zero-thermo-fluid-dynamic approach. In this way, a physical representation of the entire ORC-based unit is performed allowing also to define an optimal control strategy for maximizing plant performance under severe off-design and transient conditions.

KEYWORDS: Recuperative solar ORC-based power unit; Domestic micro-cogeneration; Scroll Expander; Theoretical model of micro-cogenerative ORC-based power unit; Plate Heat Exchanger;

1. Introduction

One of the most promising solutions to decarbonize the building sector, whose energy demand is continuously increasing [1], is combined heat and power (CHP) generation using solar thermal energy.

[1] fabio.fatigati@univaq.it

Solar energy is one of the most abundant [2] and easily accessible [3] sources of renewable energy: a system for exploiting it is to convert solar thermal radiation to thermal energy through solar collectors [4] and thermal energy to electricity via a bottoming power cycle. An Organic Rankine Cycle (ORC)-based unit is the most effective technology for generating electricity from medium- to low-temperature thermal sources [5], due to its stability and flexibility [6], simple layout, and low maintenance requirements [7]. Both solar energy availability and thermal energy demand vary during the operating time of the system [8]: the time lag between thermal energy demand and availability requires the presence of thermal energy storage (TES) [9]. The upper thermal source can supply domestic hot water or recharge the thermal storage tank, which is one of the main subsystems of the plant [10] as it enables the unit to meet variable electricity and heat demands [11].

In recent years, the solar-based ORC technology has been the subject of numerous studies, many of which have focused on the choice of working fluid and components [12]: Tzivanidis et al. [13] carried out a thermo-economic analysis of an ORC plant considering nine different working fluids; Yang et al. [14] proposed an energy, economic and environmental analysis of an ORC unit considering three low-GWP working fluids; Sonsaree et al. [15] compared the power obtained and the environmental and economic impact of a small-scale ORC-based unit considering three types of non-concentrating solar collectors. Many studies have also focused on parameters optimization, control strategies, and improved plant architectures: Cioccolanti et al. [16] investigated the overall performance of a prototype ORC plant with a phase change material storage tank; Ochoa et al. [17] evaluated the energy, environmental, and economic performance of two different configurations, basic and recuperative; Javed et al. [18] compared the energetic and economic performance of three different ORC plant configurations (regenerative, recuperative and basic) with four working fluids. Despite theoretical and numerical analysis assessed that the effects of the recuperative preheating allow the introduction of significant thermodynamic and economic benefits, few experimental analysis on this topic have been provided, [19]. In [19] it was experimentally assessed that with recuperative preheating a 9.9% increase in thermal efficiency can be achieved while producing the same power. This is particularly important in CHP applications because of the limited enthalpy content of the hot source.

In order to contribute to enrich the experimental knowledge on the benefits introduced by the recuperative stage in the ORC-based power unit, an extensive experimental campaign was conducted on an ORC-based test bench developed to bottom flat plate solar thermal collectors in microcogenerative applications. A 135 L TES was adopted to overcome the high variability of solar thermal source and the variation of Domestic Hot Water demand. The solar source was simulated by adopting two electric resistances (12 kW each) so that the time required to heat the hot water stored in the TES was feasible to perform a wide range of laboratory tests. Hence, two modes of operation, the baseline mode and the recuperative mode, were examined to compare operating conditions, efficiency and power. The extensive experimental database allows validation of a numerical model of the entire ORC unit developed to support the experimental analysis. The model allows to accurately reproduce the real plant performance, so once validated, it was adopted as a software platform to optimize the ORC-based power unit.

2. Material and Methods

2.1 Experimental layout

In the experimental layout shown in Figure 1, two 12 kW electric heaters (a) heat the water in a 135 L Thermal Energy Storage (TES) tank (b) simulating solar radiation. The tank is pressurized with air to avoid evaporation of the water, whose circulation outside the tank is entrusted by a dedicated motor-driven pump (p). The working fluid (R245fa) enters the condition of superheated vapor in the scroll expander (h) after receiving heat from the water in the evaporator (c): the mechanical power produced by the scroll expander is converted into electricity, dissipated on a rheostat-adjustable electric load. The ORC unit can operate according to two configurations, basic and recuperative. In the

first case, the working fluid leaving the expander enters the condenser (l) directly and is cooled by the tap water. Downstream of the condenser, a 3 L tank (m) acts as an oscillations damper; finally, a diaphragm pump (e) driven by an asynchronous electric motor with inverter returns the fluid to the evaporator. In the recuperative configuration (Figure 2), the working fluid leaving the expander does not enter the condenser but the recovery heat exchanger (i), where it preheats the working fluid from the pump before entering the evaporator. The switch from the basic to the recuperative configuration is carried out by opening a dedicated three-way valve.

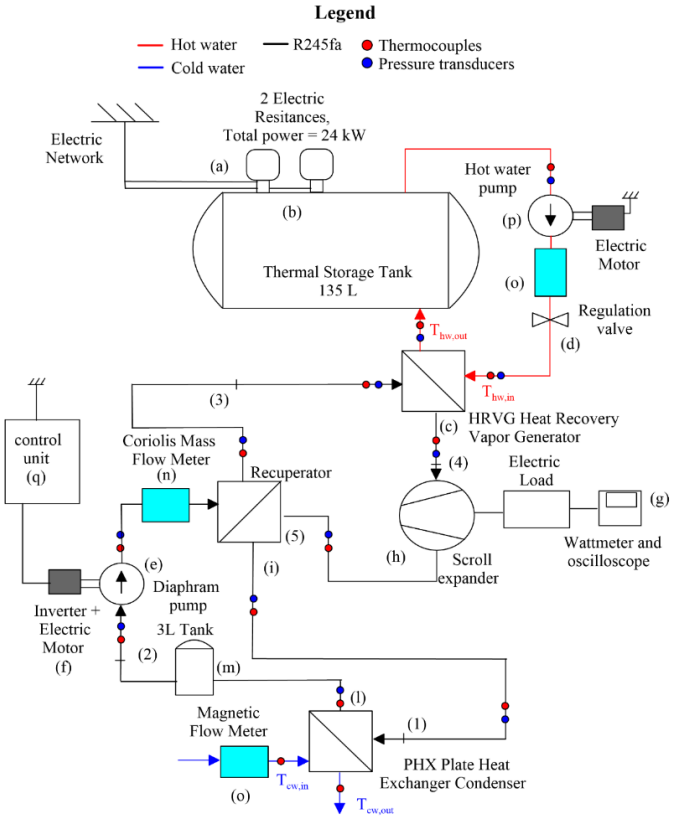

Fig. 1. ORC-based unit configuration.

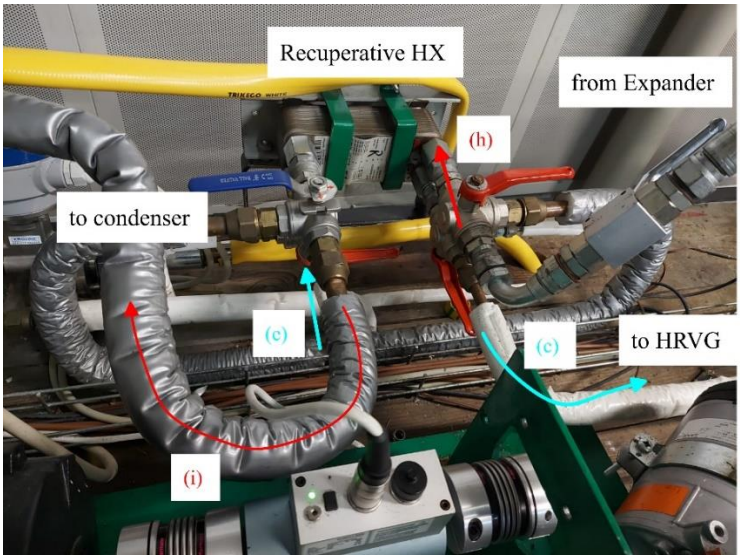

Fig. 2. RORC unit configuration.

The hot water mass flow rate entering the evaporator is adjustable via a valve (d): the variable thermal load on the evaporator allows for simulation of the fluctuations in the solar radiation availability occurring during the day. The working fluid mass flow rate is adaptable by changing the pump rotation speed; the expander rotation speed is not adjustable since it depends on the dynamic equilibrium of the shaft, which is the same for the expander and generator.

The bench is fully instrumented: there are pressure and temperature sensors at the inlet and outlet of each component, a Coriolis flowmeter (n) for measuring the working fluid mass flow rate, two magnetic flowmeters (o) for reading the mass flow rates of the cold and hot water entering respectively the condenser and the evaporator, a wattmeter (g) for measuring the power of the expander, an optical probe in the scroll casing for measuring rotational speed, which transmits the signal to an oscilloscope. Table 1 summarizes the measurement uncertainties.

An experimental campaign was performed to compare the unit performance in the two configurations under steady conditions.

Table 1: Measurement uncertainties

Variable	Sensor Type	Measurement uncertainty
Temperature	Thermocouple	± 0.75°C
Pressure	Pressure transducers	± 1.5% of full-scale
Mass flow rate (R245fa)	Magnetic Flow meter	± 0.15% measured value
Mass flow rate (water)	Magnetic Flow meter	± 0.5% measured value
Expander and Pump Power	Wattmeter	± 1% measured value
ORC efficiency		1.7%

2.2 Theoretical model

The model of the ORC power plant was reported in Figure 3 and it was developed in GT-Suite™ environment thus following an integrated zero and mono-dimensional thermo-fluid-dynamic analysis approach. The approach adopted in [20] was followed adapting the model for a lower scale ORC based power unit and introducing the recuperative section.

The pump was modelled through a look-up table as the model environment does not allow to adopt a physical model as well as for the expander (d) [23]. On the other hand, the Heat Recovery Vapor Generator (HRVG) (c), the recuperator (b) and the condenser (e) can be modelled through physical model following the same approach of [23].

The software platform ensures an accurate reproduction of the heat exchanger geometry, layout and material. Concerning HRVG model, it is divided in *Master* and *Slave* sections thermally connected [21]. The *Master* section represents the heat transfer between the working fluid and the HRVG whereas the *Slave* section takes into account the fluid boundary conditions on the opposite surface of the HRVG. HRVG is discretized in multiple flow volumes and thermal mass components connected in series or in parallel according to the considered configuration. Each flow volume sub-elements are connected to thermal masses which thermally interact with fluid sub-volumes on either side.

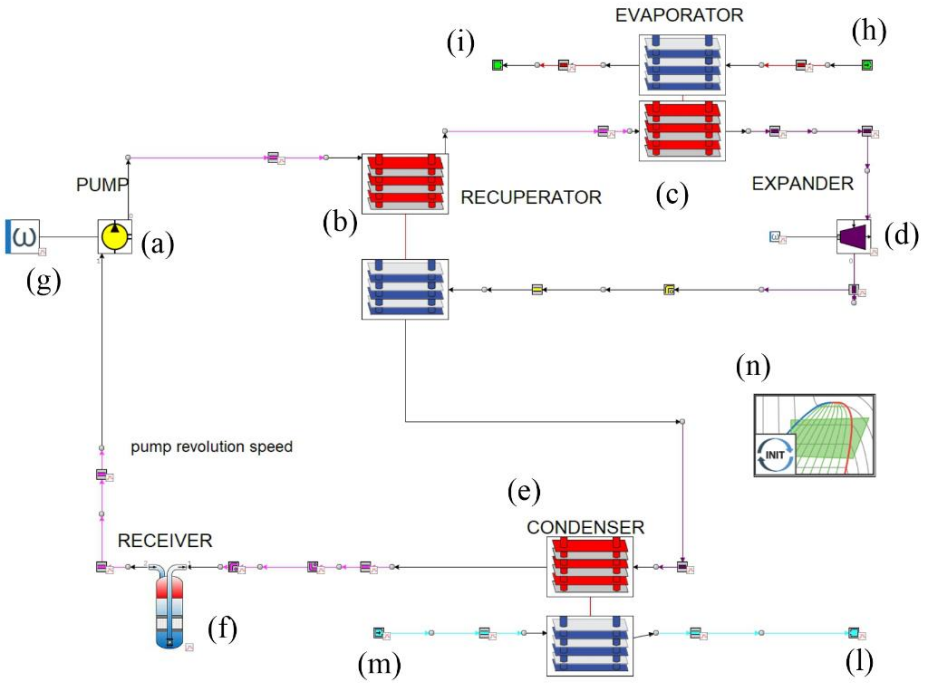

Figure 3: ORC-based power unit model

Concerning the heat transfer coefficient, the correlations of Dittus-Boelter [22] were used for the single phase and supercritical case. For the two-phase case, Plate, Yan, Lio, Lin [23] correlation was used for the condensation, whereas Plate Kandlikar [24] for evaporation. Through element (f), the 3 L plenum upstream the pump can be modelled, while element (n) allows considering the working fluid mass charge and the initial conditions. Concerning the boundary conditions, through element (g) the pump speed can be introduced to set the desired mass flow rate. The inlet temperature and mass flow rate of the hot source are introduced through the element (h), whereas through the component (i) the outlet pressure can be entered. Similarly, the mass flow rate and temperature of the cold source are introduced in element (m), whereas component (l) fixes the outlet pressure. It is worth noting that for

the considered plant architecture the expander speed is not externally imposed but depends on the equilibrium on the shaft. A linear dependence of the speed with the working fluid mass flow rate and, consequently, on the pump speed is observed. Therefore, this experimental law was introduced inside the model to consider this dependence. Consequently, in the case considered, the expander speed cannot be assumed as a boundary condition. Nevertheless, the model structure also allows this possibility to be handled in the case where the expander speed is externally imposed.

3. Results

3.1 Experimental results

The experimental analysis was performed on the ORC-based plant with (RORC) and without (ORC) the regeneration stage under steady-state operating conditions over a wide range of working points. During the experimental analyses, the electric heaters were switched off to simulate the absence of solar radiation: the energy content of the hot water feeding the evaporator from the tank is not restored and gradually erodes as the tests progress. The reduced energy availability at the upper thermal source corresponds to a reduced need for the mass flow rate of the working fluid, which under steady-state conditions is reduced by acting on the pump rotation speed.

In Figure 4(a) the RORC and ORC powers (1) are reported. It can be seen that the power values of the ORC unit in the recuperative configuration are higher than those in the non-recuperative configuration for the entire range of mass flow rates (Figure 4(a)): the maximum power values in the two cases are 380 W and 320 W respectively, but if the RORC-based unit value is obtained with a working fluid mass flow rate of 43.5 g/s, the ORC-based unit requires a mass flow rate of 48 g/s. Moreover, for the same mass flow rate, the power values obtained from the RORC-based unit system are higher by percentages, increasing from about 20 to 40% as the mass flow rate increases.

$$P_{(R)ORC} = P_{exp} - P_{pmp} \quad (1)$$

$$\eta_{(R)ORC} = \frac{P_{(R)ORC}}{\dot{m}_{HW}\, c_{\,p,HW}\left(T_{HW,\,in} - T_{HW,\,out}\right)} \quad (2)$$

This is because RORC-based unit has the best performance in terms of power thanks to the expander (Figure 4(b)), as the power values absorbed by the pump do not depend on the plant configuration but only on the mass flow rate of the working fluid, as Figure 4(c) shows. The power values of the expander in both cases are included within the same range of 300-550 W, but the curve relating to the ORC unit is shifted to the right: with the same mass flow rate, the power obtained by the RORC expander is greater. Furthermore, as the mass flow rate increases, the electrical power absorbed by the pump rises: this is why the curve relating to the ORC system power (Figure 4(a)) is not only moved to the right but also shifted downwards.

It is worth noticing as the mass flow rate for RORC-based unit and ORC-based are defined to have a comparable maximum temperature (Figure 5(a)) and consequently a similar superheating degree (Figure 5(b)) of working fluid exiting the evaporator. Figure 5(a) reports the maximum temperature of the working fluid as a function of the mass flow rate. Hence, for a given temperature the mass flow rate of working fluid is lower in the case of RORC-based unit.

The adoption of the regeneration stage ensures to reduce the thermal power needed by the hot source for a given working fluid mass flow rate. As can be seen from Figure 6(a), the thermal power of the hot source in case of RORC-based unit increases from 6.5 up to 10 kW whereas in ORC-based unit from 8 up to 12.5 kW. Thus, keeping the working fluid mass flow rate constant, the thermal power of the hot source is always lower in RORC-based unit. This is due to the thermal power

internally recovered through the recuperative plate heat exchanger. As a result, the plant efficiency (Figure 6(b)) (2) of the recuperative unit is higher over the entire mass flow rate range due to the lower thermal load at the evaporator, where the working fluid enters after being preheated in the recovery heat exchanger. The efficiency values of the case of recuperative unit vary between 4-5% in the range of flow rates considered, while those of the ORC are between 3-4%. The maximum efficiency – 5% and 4.1% respectively – occurs in both cases at a mass flow rate value of about 40 g/s which corresponds to the design operating conditions. Therefore, the plant efficiency improves up to 25% with the adoption of the recuperative stage, in agreement with what has been observed in experimental analyses reported in the literature, [19].

The amount of the thermal power exchanged at recuperative heat exchanger can be seen in Figure 7. Figure 7(a) reports the thermal power absorbed by the working fluid in the recuperative heat exchanger and in correspondence of the evaporator. Its impact on the total thermal power recovered by the working fluid is reported in Figure 7(b) where it can be seen as this percentage varies between 14 and 18% reaching a maximum in correspondence of the design point (40 g/s). It interesting to observe how the maximum efficiency is achieved in correspondence to the operating conditions in which the maximum impact of thermal power recovered at recuperative heat exchanger is achieved.

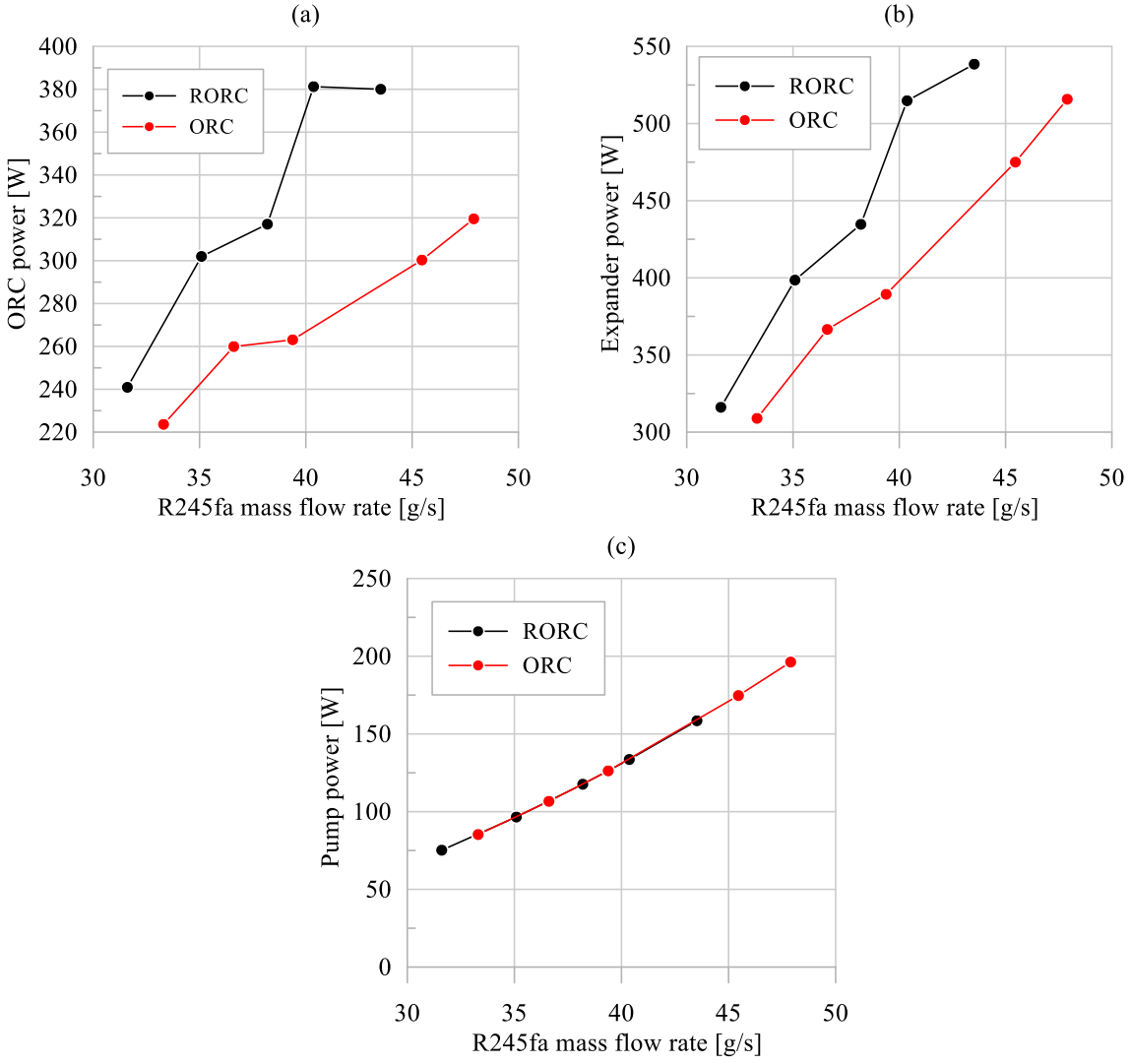

Fig. 4. ORC power (a), expander (b) and pump (c) power as a function of mass flow rate.

In Figure 8(a) the working fluid temperature at inlet and outlet side of HRVG are reported in the case of the recuperative or the simple recovery unit. It can be observed as with the adoption of the regeneration stage the temperature of the working fluid entering the evaporator varies from 40°C up to 50°C whereas in baseline ORC case is always lower than 20°C. Such benefits allow to reduce the thermal power needed by the working fluid in presence of a recuperative stage. Recuperative stage introduction allows also to reduce the temperature of the working fluid at condenser inlet (30 °C) with respect the ORC case (50-70°C). This plays a positive benefit on the reduction of plant minimum pressure thanks to the lower thermal power to exchange at condenser in presence of a recuperative stage. Indeed, in Figure 9(a) it can be seen how in this case minimum pressure is lower than the one achieved in the case without recuperative stage.

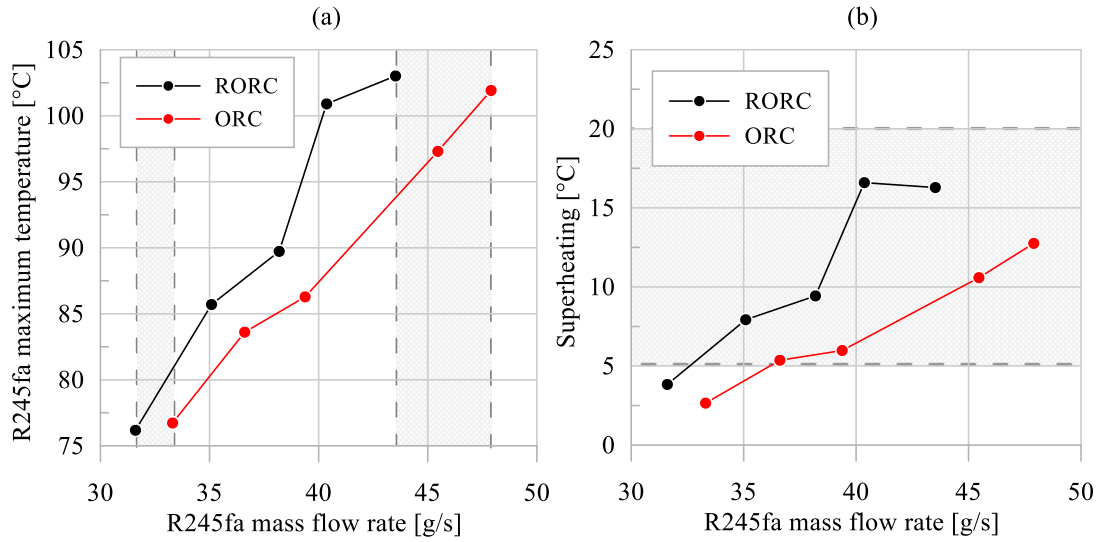

Fig. 5. R245fa maximum temperature (a); superheating degree at the evaporator outlet (b).

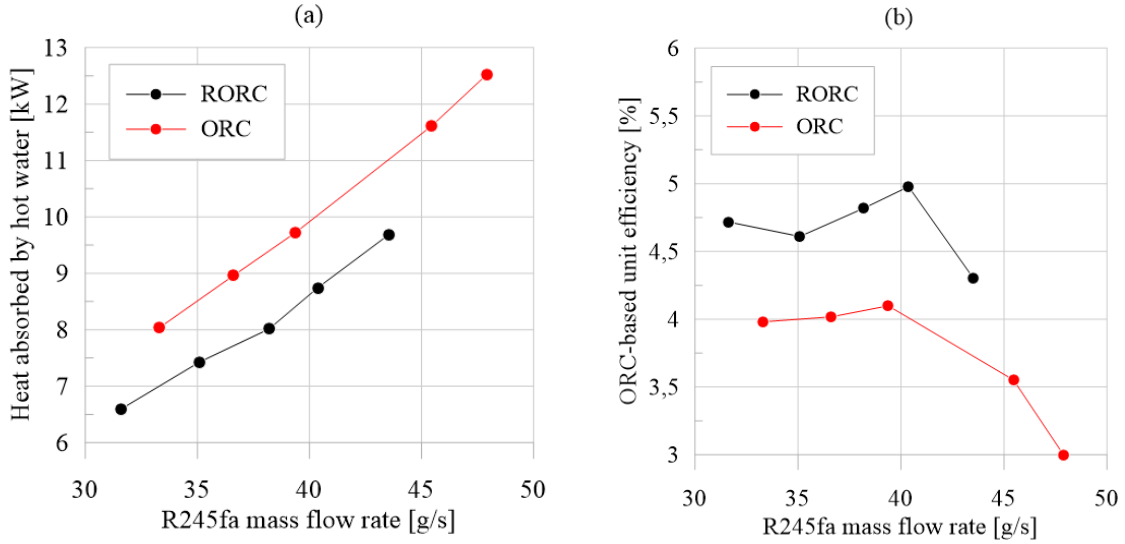

Fig. 6. Heat absorbed by hot water (a); ORC-based unit efficiency (b).

Concerning the maximum pressure, linear relation of the pressure increase with mass flow rate is the same in the two recovery units. This is in accordance to the permeability law which puts in relation the ORC maximum pressure and the working fluid circulating inside the system, [26]. It was seen as this property is defined by volumetric expanders. Indeed, permeability α is defined as the attitude of a volumetric machine to be crossed by the working fluid, hence, it can be expressed as the ratio of the working fluid mass flow rate and the expander pressure difference between intake and exhaust side (3).

$$\alpha = \frac{\dot{m}_{WF}}{\Delta p_{exp}} \quad (3)$$

It was seen that the higher is the expander permeability the lower is the ORC maximum pressure for a given working fluid mass flow rate. Indeed, volumetric expander behaves as a revolving valve. Observing Figure 9(b), despite the ORC-based unit maximum pressure growth with mass flow rate is the same, the maximum pressure is different in RORC- and ORC-based cases. Indeed, in the first case the working fluid mass flow rate is lower for a given working point thanks to the introduction of recuperative stage.

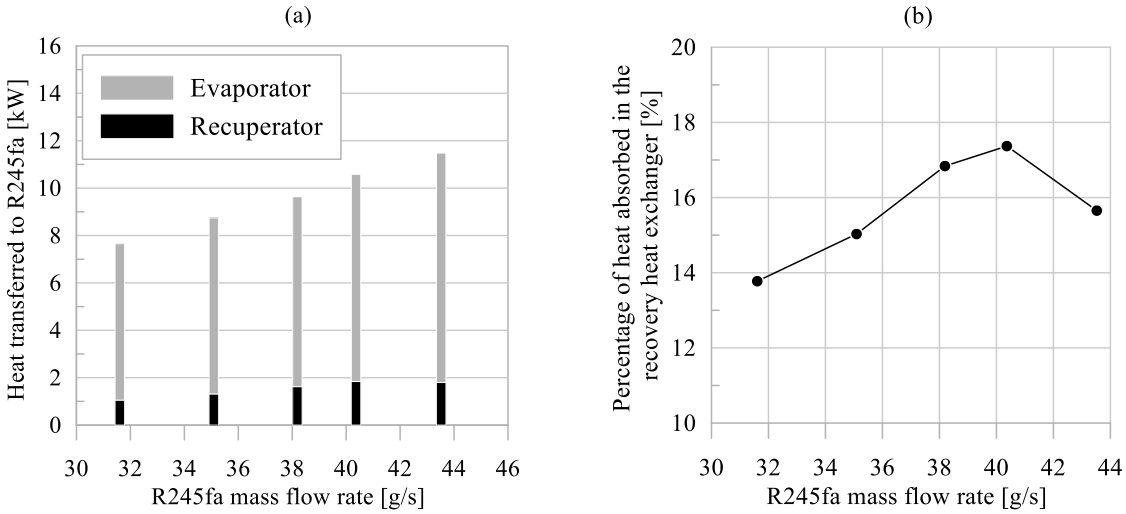

Fig. 7. Thermal power absorbed by the working fluid (a) and percentage of heat absorbed in the recuperator (b).

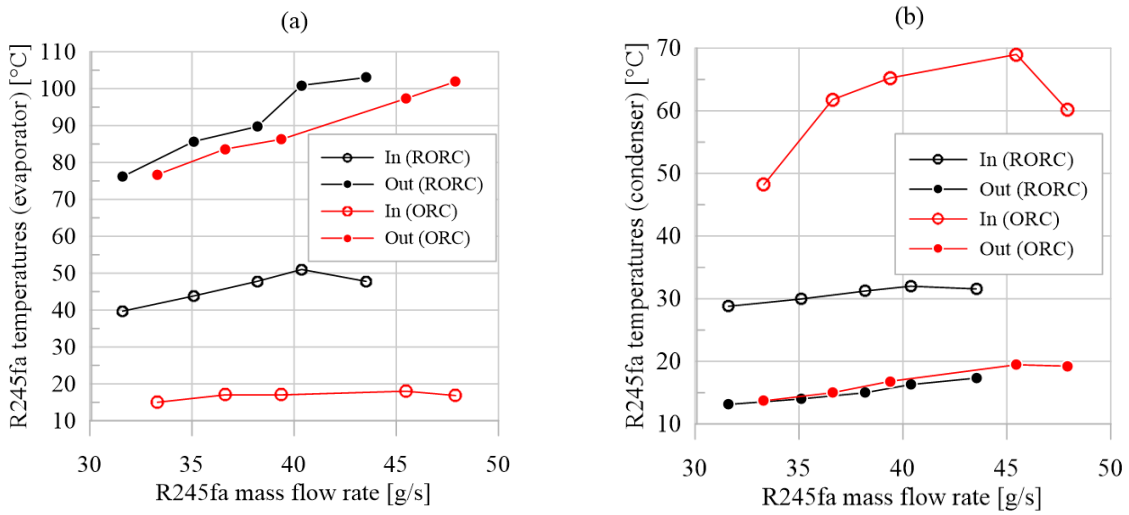

Fig. 8. R245fa temperatures in the evaporator (a) and condenser (b).

Considering for instance the point at which the working fluid has the highest temperature (100°C), the working fluid mass flow circulating within the plant is 40 g/s and 45 g/s in the case of a recuperative and of a simple cases, respectively. This means that RORC-based unit has a maximum pressure of 9.5 bar whereas that of the ORC-based unit is 10.5 bar. Reducing the maximum pressure yields benefits not only on the expander efficiency (and consequently on the whole plant efficiency), but it also brings an economic benefit as the plant material faces lower mechanical stresses. In addition, although the ORC maximum pressure is lower in RORC case, reducing the ORC minimum pressure prevents this reduction in pressure ratio from affecting the power output of the expander, as can be seen in Figure 4(b).

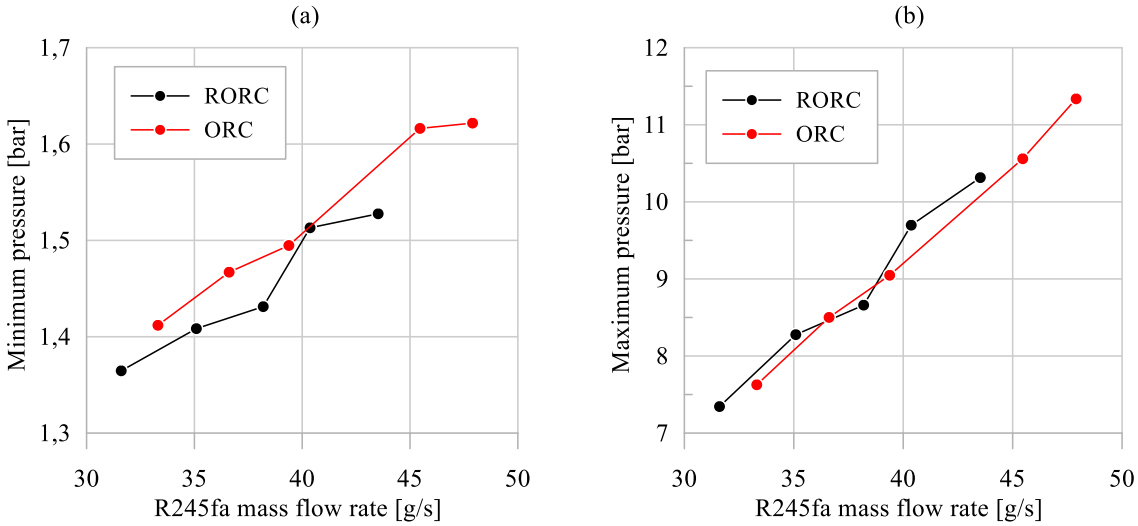

Fig. 9. Minimum (a) and maximum (b) plant pressures.

Such results demonstrate the suitability of recuperative stage adoption in the case in which the plant is driven exclusively by the thermal power stored in TES. Indeed, the higher plant efficiency obtained in presence of a recuperative stage allows involves a slower decrease of the temperature of hot water stored in TES thus providing a higher power produced during the plant activation.

3.2 Model Validation

Thanks to the wide experimental data set (Table 2), the model of the ORC-based plant was validated to demonstrate their accuracy. In Table 3 the errors between the experimental and theoretical data are reported for the main quantities analyzed. Concerning the working fluid mass flow rate, the maximum relative errors are equal to -1.8% whereas for ORC maximum pressure and temperature maximum relative errors are respectively equal to -2.7% and 10.5%.

Table 2: Experimental quantities

Experimental quantities	**Units**	**1**	**2**	**3**	**4**	**5**	**6**
mass flow rate	g/s	50.7	45.9	41.4	49.3	17.8	23.0
Unit maximum pressure	bar	10.4	9.7	9.0	10.1	5.0	5.9
Unit maximum temperature	°C	108.0	104.3	105.9	104.3	91.4	90.5
Unit minimum pressure	bar	1.5	1.5	1.4	1.5	1.2	1.3
Unit minimum temperature	°C	20	20.2	17.8	23	14.6	13.7
Temperature at RHX inlet (hot side)	°C	82	65.6	76.7	78.3	69.2	67.7
Temperature at RHX outlet (hot side)	°C	33	30.3	31.1	34.8	29	28.4
Temperature at RHX outlet (cold side)	°C	53.3	44.2	50.3	53.0	44.6	42.9
Expander power	W	583	565	546	563	271	347
ORC unit power	W	360	386	404	354	256	314

For what regards the ORC maximum and minimum temperature the maximum absolute errors are respectively equal to -5°C and 9.6°C. The maximum absolute errors of the hot side inlet and outlet temperature at the regenerator are equal to 5.7°C and 4.5°C. On the other hand, the modelled cold side outlet temperature differs by 6.1°C. Hence, the low maximum errors demonstrate the robustness of the model in the prediction of the whole behavior of the ORC plant. Consequently, the model can catch the ORC plant performance in terms of power and efficiency with maximum relative errors of -14.7 % and 10.7% respectively. Hence, the model accuracy can be retained satisficing considering the wide operating range analyzed.

Table 3: Errors between experimental and theoretical data

errors	**1**	**2**	**3**	**4**	**5**	**6**
mass flow rate [%]	-1.0	-0.9	-1.3	-0.4	-1.6	-1.8
ORC maximum pressure [%]	-1.9	-0.1	-0.2	-2.7	-2.1	-1.8
ORC maximum temperature [°C]	-1.6	2.5	1.6	-5.0	0.8	0.7
ORC minimum pressure [%]	1.5	-1.2	0.6	-4.9	9.3	10.5
ORC minimum temperature [°C]	5.3	4.5	6.6	2.1	8.2	9.6
Temperature at RHX inlet (hot side) [°C]	-1.8	5.7	2.0	-5.3	2.9	2.3
Temperature at RHX outlet (hot side) [°C]	4.2	4.2	4.5	0.5	2.5	3.3
Temperature at RHX outlet (cold side) [°C]	2.0	6.1	4.3	-1.8	6.9	7.3
ORC unit power [%]	-5.4	-3.8	-10.0	-11.7	-12.7	-14.7

ORC efficiency [%]	4.4	2.5	9.2	11.4	9.0	10.7

3.3 Theoretical results

Once the theoretical model was validated, it was used as a software platform to develop operating map for a wide set of working conditions. The RORC-based unit power and efficiency are evaluated when the hot water flow rate varies from 6 L/min up to 18 L/min and the hot water temperature changes from 90°C and 110°C. The aim of this analysis is to find how to operate the RORC unit under severe off-design conditions typical of the analysed application.
In Figure 10(a), the RORC unit power is reported as a function of working fluid WF mass flow rate for different hot water flow rate Q_{HW} when the hot water HRVG inlet temperature is equal to 100 °C. It can be observed as the RORC power trend assumes a maximum for a WF mass flow rate which increases with Q_{HW}. Indeed, when Q_{HW} increases from 6 L/min up to 18 L/min the WF mass flow rate allowing to achieve the maximum RORC power grows from 38 g/s up to 45 g/s. This is due to the fact that the higher is the Q_{HW} the larger is the thermal power available for the RORC unit for a given $T_{HW,in.}$ Therefore, to ensures that the working fluid enters the expander with a proper superheating degree (15-20 °C) the mass flow rate should be increased with Q_{HW}. It is important to observe that with Q_{HW} also the RORC unit maximum power increases. Indeed, maximum RORC power grows from 300 W up to 400 W when Q_{HW} ranges from 6 L/min up to 18 L/min. Anyway, the difference of maximum RORC power between the case when QHW is respectively equal to 12 L/min and 18 L/min is low as the maximum RORC power are respectively equal to 360 W and 400 W. Moreover, also the operating range in which the RORC power is higher than 200 W is similar. Therefore, when the plant is driven exclusively by TES hot water in absence of solar power restoring the TES enthalpy content, Q_{HW} should be set equal to 12 L/min. Indeed, this choice allows to reduce the TES temperature decrease rate thus enhancing the RORC operating time.

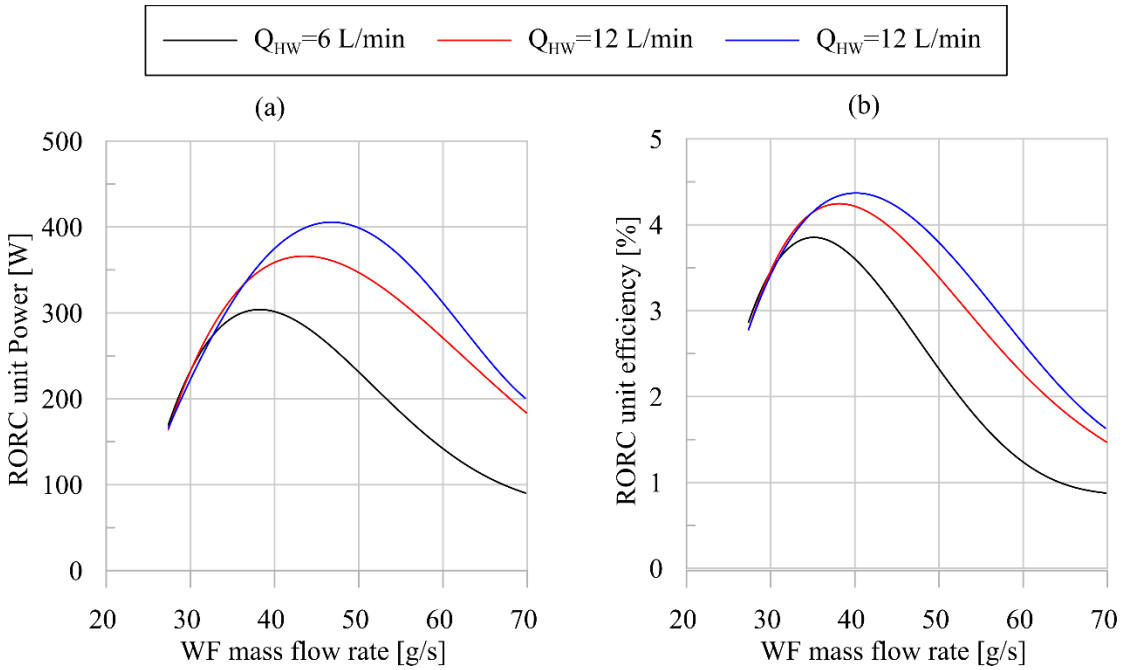

Fig. 10. RORC-based unit power (a) and efficiency (b) as a function of flow rates of working fluid and hot water.

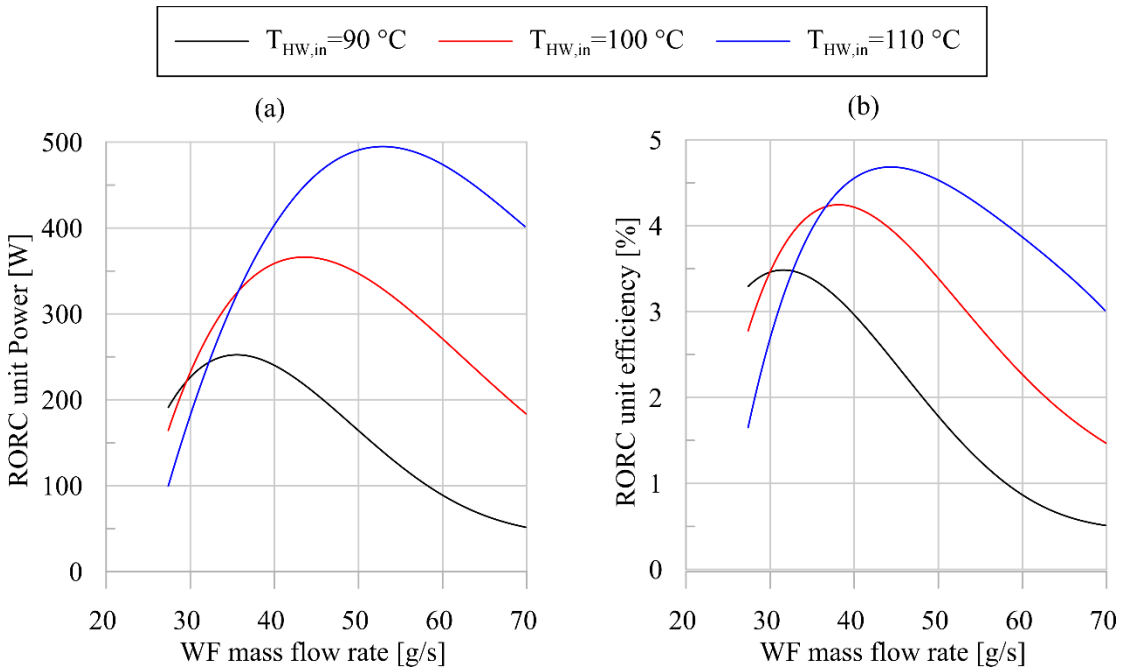

Fig. 11. RORC unit power (a) and efficiency (b) as a function of flow rate of working fluid and hot water temperature at HRVG inlet.

The RORC-based unit efficiency presents a similar behaviour of that observed for the power. The only difference is that the maximum efficiency is achieved for a slightly lower mass flow rate with respect to the case of RORC power. For instance, the WF mass flow rate maximizing the RORC unit efficiency is 40 g/s when Q_{HW} is 18 L/min. Under the same conditions, the WF mass flow rate that maximizes the ORC power is equal to 45 g/s. However, these mass flow rates are close, so an intermediate mass flow rate can be chosen to optimize both the power and efficiency of the unit without a regeneration stage.

A similar analysis was conducted also varying the $T_{HW,in}$ keeping constant the Q_{HW} to 12 L/min. Also in this case, the RORC power produced by the unit (Figure 11(a)) and the efficiency has a maximum value increasing with $T_{HW,in.}$ Moreover, the WF mass flow rate for which the RORC power is achieved grows with $T_{HW,in}$. As matter of fact, when $T_{HW,in}$ grows from 90°C up to 110°C the RORC maximum power raises from 250 W up to 500 W. The same applies for RORC-based unit efficiency as it grows from 3.5% up to 4.5% when $T_{HW,in}$ increases from 90°C up to 110 °C. Similarly to the previous case, also when $T_{HW,in}$ was varied the WF mass flow rate allows to achieve the maximum power and efficiency are not the same but are closer. An important aspect to remark is the variation of $T_{HW,in}$ produces a higher variation on both RORC unit power and efficiency. Therefore, from the point of view of sensitivity analysis, the $T_{HW,in}$ variation plays a greater impact on the RORC performance than Q_{HW} . Consequently, Q_{HW} should be reduced as much as possible to delay the $T_{HW,in}$ reduction when the plant is exclusively driven by the TES tank.

4. Conclusions

This paper reports the results of experimental tests conducted on a small-scale ORC-based unit for solar micro-cogeneration to compare the performance in terms of power and efficiency of the basic configuration (ORC) with the regeneration stage (RORC). RORC is obtained favoring a thermal

recovery between the working fluid leaving the expander and the same fluid leaving the pump before it enters the evaporator (HRVG). The unit was fed by the hot water inside the reservoir which is usually inserted in conventional flat plate solar collectors. The testing activity was done without restoring the energy inside the reservoir, being finalized to use the hot water available to produce electrical energy after having fulfilled the hot water demand for domestic use. According to this choice, the hot water temperature decreases as the electrical energy generation proceeds, entraining the unit to even more severe off design conditions. Experimental data show that:

1. Since the hot water enters the evaporator at higher temperatures in the RORC configuration, the RORC system operates with a lower R245fa mass flow rate: it varies between 31 and 43 g/s in the RORC unit and between 48 and 33 g/s in the ORC unit;

2. For the same working fluid mass flow rate, the power obtained by the expander in RORC mode is higher, the degree of superheating and the maximum cycle temperature being higher. The electricity absorbed by the pump depends only on the mass flow rate of the working fluid and not on the type of configuration.

3. The power obtained at the same mass flow rate of R245fa is always higher for the RORC configuration: for a working fluid mass flow rate of 40 g/s, which is the value in the design condition, the power obtained by the RORC unit is 380 W, that obtained by the ORC unit is about 270 W.

4. The efficiency of the RORC-based unit is higher throughout the range of mass flow rates considered, since the working fluid arrives preheated in the evaporator: at 40 g/s, the efficiency is 5% for the RORC unit and 4% for the ORC unit.

The extensive experimental data set allows validation of a theoretical plant model developed in the GT-Suite™ environment. The low errors between experimental data and predictions demonstrate the suitability of the model to be acted as a software platform for plant optimization.

Once validated, the model was used as a software platform to analyze the RORC behavior under a wide set of operating conditions. The RORC-based unit can produce up to 500 W with an efficiency of 4.5 % when the hot water temperature at the HRVG inlet is 110 °C and the flow rate is 12 L/min. In addition, variations in hot water temperature (90°C-110 °C) have a greater effect on the power and efficiency of the RORC than changes in Q_{HW} (6 L/min -18 L/min). Therefore, Q_{HW} should be reduced as much as possible to delay the decrease in $T_{HW,in}$ when the RORC-based unit is supplied exclusively by the TES tank in the absence of solar power.

Nomenclature

Symbols

(a) Electric resistances
(b) TES- Thermal Energy Storage Tank
(c) HRVG- Heat Recovery Vapor Generator
(d) Regulation valve
(e) Working fluid pump
(f) Pump electric motor and inverter
(g) Wattmeter and oscilloscope
(h) Scroll Expander
(i) Recuperator

η- efficiency
ρ-density [kg/m^3]

Subscripts

exp-expander
HW- Hot water
HRVG- Heat Recovery Vapor Generator
in-inlet
ORC-Organic Rankine Cycle

(l) condenser
(m) 3 liters tank
(n) Coriolis Mass flow meter
(o) Magnetic flow meters
(p) hot water pump
c_p -Specific heat at constant pressure [J/(kgK)]
$\dot{m}$ - mass flow rate [kg/s]
P- Power [W]
p-pressure [Pa]-[bar]

Greek letters
α- permeability [kg/(s·MPa)]
Δp-pressure difference [bar]

out-outlet
pmp- pump
wf-working fluid

Achronyms
WF-working fluid

HRVG-Heat Recovery Vapor Generator
ORC-Organic Rankine Cycle
PHX- Plate Heat Exchanger
HW- Hot Water
RHX- Recuperative Heat Exchanger
RORC- Organic Rankine Cycle with recuperative stage
WF-Working fluid

Acknowledgment

The authors are grateful to SIVAM S.p.A for the support given in this activity. New subroutines employed in the ORC unit model were developed in the framework of the European project Development of efficient and environmental friendly LONG distance powertrain for heavy duty trucks and coaches: LONGRUN GRANT AGREEMENT NUMBER 874972.

References

[1] Rodriguez-Pastor D A, Becerra J A and Chacartegui R 2023 Adaptation of residential solar systems for domestic hot water (DHW) to hybrid organic Rankine Cycle (ORC) distributed generation *Energy* **263** 125901

[2] Roumpedakis T C, Loumpardis G, Monokrousou E, Braimakis K, Charalampidis A and Karellas S 2020 Exergetic and economic analysis of a solar driven small scale ORC *Renew. Energy* **157** 1008-1024

[3] Shahverdi K, Loni R, Ghobadian B, Monem M J, Gohari S, Marofi S and Najafi G 2019 Energy harvesting using solar ORC system and Archimedes Screw Turbine (AST) combination with different refrigerant working fluids *Energy Convers. Manage* **187** 205-220

[4] Ashwni and Sherwani A F 2022 Analysis of solar energy driven organic Rankine cycle-vapor compression refrigeration system *Thermal Sci. Eng. Prog.* **35** 101477

[5] Bellos E and Tzivanidis C Investigation of a hybrid ORC driven by waste heat and solar energy 2018 *Energy Convers. Manage.*, **156** 427-439

[6] Bai M, Zhang Y, Deng S, Zhao L, Zhao R and Lu Y 2020 An experimental study on operation characteristics of the organic Rankine cycle system under the single-and multiple-variables regulation *Sustain. Energy Technol. Assess.* **41** 100785

[7] Yu H, Helland H, Yu X, Gundersen T and Sin G 2021 Optimal design and operation of an Organic Rankine Cycle (ORC) system driven by solar energy with sensible thermal energy storage *Energy Convers. Manage.* **244** 114494

[8] Tashtoush B and Algharbawi A B R 2019 Parametric study of a Novel Hybrid Solar Variable Geometry Ejector cooling with Organic Rankine Cycles *Energy Convers. Manage.* **198** 111910

[9] Zairi A, Mokhtari A M, Menhoudj S, Hammou Y, Dehina K and Benzaama M H 2021 Study of the energy performance of a combined system: Solar thermal collector – Storage tank – Floor heating, for the heating needs of a room in Maghreb climate *Energy Build.* **252** 111395.

[10] Permana D I, Rusirawan D and Farkas I 2022 A bibliometric analysis of the application of solar energy to the organic Rankine cycle *Heliyon* **8** (4)

[11] Peacock J, Huang G, Song J and Markides C N 2022 Techno-economic assessment of integrated spectral-beam-splitting photovoltaic-thermal (PV-T) and organic Rankine cycle (ORC) systems *Energy Convers. Manage.* **269** 116071

[12] Nguyen V N, Pham N D K, Duong X Q, Tran V D, Pham M T, Rajamohan S, Cao X T and Truong T H 2023 Combination of solar with organic Rankine cycle as a potential solution for clean energy production *Sustain. Energy Technol. Assess.* **57** 103161

[13] Tzivanidis C, Bellos E and Antonopoulos K A 2016 Energetic and financial investigation of a stand-alone solar-thermal Organic Rankine Cycle power plant *Energy Convers. Manage.* **126** 421-433

[14] Yang J, Gao L, Ye Z, Hwang Y and Chen J 2021 Binary-objective optimization of latest low-GWP alternatives to R245fa for organic Rankine cycle application *Energy* **217** 119336

[15] Sonsaree S, Asaoka T, Jiajitsawat S, Aguirre H and Tanaka K 2018 A small-scale solar Organic Rankine Cycle power plant in Thailand: Three types of non-concentrating solar collectors *Solar Energy* **162** 541-560

[16] Cioccolanti L, Tascioni R, and Arteconi A 2018 Mathematical modelling of operation modes and performance evaluation of an innovative small-scale concentrated solar organic Rankine cycle plant *Appl. Energy* **221** 464-476

[17] Ochoa G V, Ortiz E V and Forero J D 2023 Thermo-economic and environmental optimization using PSO of solar organic Rankine cycle with flat plate solar collector *Heliyon* **9**

[18] Javed S and Tiwari A K 2023 Performance assessment of different Organic Rankine Cycle (ORC) configurations driven by solar energy *Process Saf. Environ. Protect.* **171** 655-666

[19] Eyerer S, Dawo F, Schifflechner C Niederdränk A Spliethoff H and Wieland C 2022 Experimental evaluation of an ORC-CHP architecture based on recuperative preheating for geothermal applications *Appl. Energy* **315** 119057

[20] Marchionni M, Fatigati F, Di Bartolomeo M, Di Battista D and Petrollese 2022 M Experimental and Numerical Dynamic Investigation of an ORC System for Waste Heat Recovery Applications in Transportation Sector *Energies* **15** 9339

[21] 2020 GT-SUITE-Flow Theory Manual T Gamma—Gamma Technologies, USA

[22] Dittus F W and Boelter L M 1985 Heat transfer in automobile radiators of the tubular type. *Int. Commun. Heat Mass Transf.* **12** 3–22

[23] Yan Y, Lio H and Lin T 1999 Condensation heat transfer and pressure drop of refrigerant R-134a in a plate heat exchanger *Int. J. Heat Mass Transf.* Volume **42** (6) 993-1006.

[24] Kandlikar S G 1990 A General Correlation for Saturated Two-Phase Flow Boiling Heat Transfer Inside Horizontal and Vertical Tubes *J. Heat Transf.* **112** 219–228

[25] Friedel L 1979 Improved Friction Pressure Drop Correlation for Horizontal and Vertical Two-Phase Pipe Flow.

[26] Fatigati F, Vittorini D, Coletta A and Cipollone R 2022 Assessment of the differential impact of scroll and sliding vane rotary expander permeability on the energy performance of a small-scale solar-ORC unit, *Energy Convers. Manage.* **269** 116169